FORMAL REPORT

Box

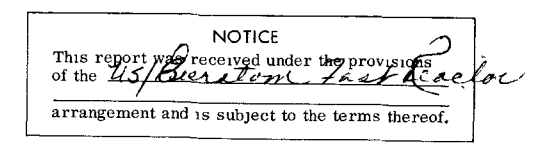
B. 111

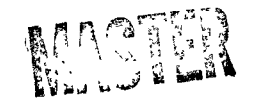
EURFNR - 1060

UNITED STATES — EURATOM FAST REACTOR EXCHANGE PROGRAM

Original report number KFK 1680					
Title Age-Hardening Phenomena in V-Ti,					
V-Ti-Si, V-Zr and V-Hf Alloys with					
Reference to the Metalloids N, O, B					
and C					
Author(s) H. Scholz					
Originating Installation					
Karlsruhe Nuclear Research Center					
Date of original report issuance October 1972					
Reporting period covered					
reporting portion of force					
Translated from the original German					
This report, translated wholly or in part from the original					
language, has been reproduced directly from copy pre-					
pared by the United States Mission to the European Atomic					
Energy Community.					

THIS REPORT MAY BE GIVEN UNLIMITED DISTRIBUTION





DISCLAIMER

Portions of this document may be illegible in electronic image products. Images are produced from the best available original document.

KARLSRUHE NUCLEAR RESEARCH CENTER

October 1972

KFK 1680

Institute for Materials and Solids Research
Fast Breeder Project

Age-Hardening Phenomena in V-Ti, V-Ti-Si, V-Zr and V-Hf Alloys with Reference to the Metalloids N, O, B and C

by Scholz

> Official Report USAEC-EURATOM Fast Neutron Reactor Exchange

Gesellschaft für Kernforschung mbll., Karlsruhe

Table of Contents

- 1. Introduction
- 2. Precipitation-Hardening Vanadium Alloys
- 3. Test Procedure
- 3.1 Test Material
- 3.2 Mechanical Examination
- 4. Results
- 4.1 Age-hardening Test
- 4.2 Tensile Tests
- 4.3 Metallographic Examination
- 5. Discussion of Results
- 6. Abstract
- 7. References

Abstract

An investigation was performed to determine the influence of N, O, B and O on the precipitation- and age-hardening-behaviour of the alloys V-Ti, V-3Ti-Si, V-2Zr and V-1Hf. The purpose of this study was to investigate what influence these interstitialas have on the age-hardening processes and whether this influence has to be taken into account for fuel element cladding. In addition, the question had to be answered whether or not there are new applications possible for age-hardened vanadium alloys beyond the field of nuclear application. The alloys V-Ti-O and V-Hf-C showed a increase in hardness after temperature treatments. A high carbon content in the alloy V-Ti-O prevents age-hardening. Age-Hardening was increased by additions of boron and silicon. The age-hardening processes can be used for a possible improvement of the creep strength to temperatures up to 750°C, as above this temperature overaging occurs after a short time. In order to avoid a too high resistance to deformation during the extrusion of V-Ti-O-alloys the extrusion temperature has to be higher than 800°C. New field of application for vanadium-base alloys beyond nuclear engineering could not be pointed out in time.

1. Introduction

Pure vanadium possesses several noteworthy properties which have justified its use as a basic metal in alloy development work over the last two decades. Pure vanadium is machinable and weldable. The density p is 5.96 g/cm³ and thus lies between that of titanium ($\rho = 4.51 \text{ g/cm}^3$) and iron ($\rho =$ 7.88 g/cm^3). The modulus of elasticity of pure vanadium is given as 12,000-15,000 kp/mm²; the melting point is 1890°C. thermal conductivity, which increases for rising temperature, is 0.047 cal/cm²/cm/°C/sec at 100°C (Ref. 1). Vanadium is one of the superconducting metals; the transition temperature T_c is between 4.3 and 5.3°K. One of the main chemical properties of vanadium is that it is insoluble in water, hydrochloric acid and alkalis. The properties which have prompted consideration of vanadium for use in reactor engineering are the low absorption cross-section on Y for fast neutrons $(\sigma n \gamma (100 \text{ keV}) = 4.5 \text{ mb}) (\text{Ref. 2}) \text{ and the}$ lack of high temperature embrittlement. A disadvantage, however, is the low corrosion resistance of the vanadium alloys, due to the low melting point of the oxide V₂O₅ (675°C). Attempts to develop alloy systems with surface oxide layers of higher melting points have had only limited success, so that the only possible alternative is to use corrosion-resistant cladding or case hardening.

The aim of the studies conducted here was to answer the question whether an increase

⁻NOTICE-

This report was prepared as an account of work sponsored by the United States Government. Neither the United States nor the United States Atomic Energy Commission, nor any of their employees, nor any of their contractors, subcontractors, or their employees, makes any warranty, express or implied, or assumes any legal liability or responsibility for the accuracy, completeness or usefulness of any information, apparatus, product or process disclosed, or represents that its use would not infringe privately owned rights.

in the strength of vanadium alloys can be achieved by precipitation hardening and whether the essential conditions are present for improving the creep rupture strength properties by age-hardening. The study also included an investigation of whether age-hardening phenomena must be taken into consideration in the production of vanadium alloy cladding tubes for sodium or heliumcooled fast breeder reactors. In conjunction with this the project included an investigation of the extent to which vanadium alloys can be contemplated for uses outside nuclear engineering.

2. Precipitation-Hardening Vanadium Alloys

Precipitation hardening is divided up into two types, depending on the chemical composition of the phases precipitated, i.e., precipitation hardening due to oxide, nitride, carbide and boride phases, which can occur in vanadium as a result of the addition of getter metals such as Ti, Zr and Hf, and also precipitation hardening due to intermetallic phases. metals whose solubility in vanadium increases with the temperature are suitable for precipitation hardening by intermetallic phases. These include Zr, Hf, Fe, Co, Ni, Al, Si, Sn and Be. Table 1 shows the solubility limits of Zr, Hf, Fe, Co, Ni, Al, Si, Sn and Be at elevated temperature in w/o. The weight fractions listed must be reached at least in order to permit the precipitation of intermetallic phases in vanadium. precipitations to be expected are also listed in Table 1. However, no precipitationhardening vanadium-rich alloys are known from the systems listed above. The strengthenhancing influence of B, C, N and O on vanadium and vanadium alloys has already been pointed out, but it is not yet clear

whether this strength enhancement is due to the solution of the elements or to the precipitation of metalloid phases.

Fig. 1, taken from D.R. Matthews, G.H. Keith and E.A. Loria (Ref. 3), shows the increase in the yield point of pure vanadium as a function of the B, N, O and C content at room temperature. The greatest increase in strength is produced by nitrogen and oxygen, which severely reduce the ductility of vanadium with a simultaneous increase in strength. Also, when N and O are added to vanadium it is not always clear whether the increase in strength is produced by the dissolved and/or the precipitated nitrides and oxides. The influence of carbon on the alloys V-60Nb-Ti, Zr, Hf and V-40, 60Nb-30, 10Ta-1Zr, Hf has been investigated by F.C. Holtz and L.B. Richard (Ref. 4). In the short-term creep test the siliconized alloy V-60Nb-10Ta-1Zr-0.075 was found to be the most creep resistant in air at a temperature of 1090°C. No further data are given in the above work on the precipitation or hardening behavior. The influence of boron and boron plus carbon on the behavior of vanadium is described by H.G. Iverson, D.R. Matthews and J.S. Winston (Ref. 5). Boron and boron plus carbon reduce the grain size of vanadium considerably (Figs. 2 and 3). The strength of vanadium is only slightly increased by boron at room temperature, but at 77°K the yield point is raised substantially by the addition of boron (Figs. 4 and 5).

It was also found that vanadium together with boron and carbon shows an increase in strength due to age-hardening (Fig. 6). However, boron alone produces hardly any increase in the strength of vanadium by

age-hardening. The influence of boron on the material behavior of vanadium-base alloys has not so far been investigated in the literature available.

3. Test Procedure

3.1 Test Material

A total of 15 vanadium-base alloys were investigated in the present work. The alloys, the composition of which is given in Table 2, can be divided up into three groups, namely, the vanadium-titanium alloys with titanium contents of 1, 3, 5, 10 and 20 % (alloy Nos. 1-5), the V-3Ti alloys with additions of silicon (Nos. 6 and 7) and the vanadium alloys with additions of 3Ti, 2Zr, 1Hf, whose oxygen and nitrogen contents were kept roughly constant, the boron and carbon being varied (Nos. 8-15). Alloys 6-15 were supplied by the Metallgesellschaft in rods 10 mm in diameter and 200 mm long. According to the suppliers the rods were subjected to 20 % cold-work in three forgings and then annealed for 1 h at 980°C in a vacuum of 10⁻⁵ torr. For the age-hardening examination the rods were annealed in a Leybold-Heraeus vacuum quenching furnace at 1250°C for 1 h under a vacuum of 2 . 10⁻⁵ torr and quenched in water. The alloys with different Ti contents (1 - 5) were rolled into sheets 1-2 mm thick after the 980 °C annealing. Titanium chips were added as getters to the sheets, which were cast into quartz tubes under a pressure of 10^{-4} torr, homogenized for 3 h at a temperature of 1100°C and quenched in water with the quartz tubes opened. The oxide layers which were present on all the alloys investigated here after the quenching operations were carefully removed.

The micrographs of the Ti-containing alloys show a segregated structure with regions of high and low titanium contents. The segregations zones can be seen as light-dark demarcated areas in the micrograph of a V-3Ti sample containing 800 ppm, which can be regarded as characteristic (Fig. 7a). The different Ti distribution was demonstrated on the basis of a scanning electron micrograph (Fig. 7b).

No segregation zones were observed in the alloys containing Zr and Hf. The grain size of the alloys containing Ti and Zr are roughly the same. However, the Hf-containing alloys display a fine-grain structure, as can be seen on the basis of a V-lHf sample containing carbon and boron (Fig. 8).

3.2 Mechanical Examination

The homogenized material was aged in airtight quartz tubes in a vacuum of 10⁻⁴ torr, together with titanium sponge as a gettering substance. In the first group of alloys, the titanium content of which was between 1 and 20 %, aging took place up to 20 days at temperatures of 400, 500, 600, 700 and The Si-containing alloys were aged at 400, 550 and 700°C. The age-hardening behavior of the third group was investigated at 250, 450, 600, 750 and 900°C. In order to rule out surface effects in the hardness measurements, the samples were thoroughly gound down. The hardness measurements were carried out using the Vickers method at a load of 30 kp. One sample was used for determining each datum point. It was found that samples of the same alloy in group 1 showed different hardness values

in the homogeneous state. In order to determine the hardness curves, the mean was therefore taken of the hardness values for the homogeneous states of each alloy; the increase in hardness due to aging were referred to these mean values. In the other alloys (2 and 3) the scatter of the hardness values was disregarded.

Tensile tests were carried out at room temperature and 350°C on the alloy V-1Ti and on alloys 8-15, which were present in different age-hardening conditions. The tensile specimens of alloy V-1Ti were in sheet form and those of the others as rods (Figs. 9a,b). An Instron electronic tensile testing machine of type TT-DM-L was employed. Argon was added as a shield gas in the tensile tests conducted at 350°C. The test temperature was kept constant to within ±2°C. The average cross-beam advance was 0.2 mm/min, correcponding to a strain rate of 1.6 · 10⁻⁴ 1/sec and 2.4 · 10⁻⁴ 1/sec for the sheet and rod specimens respectively.

4. Results

4.1 Age-hardening Tests

The age-hardening curves of group 1, containing different titanium contents, are shown in Figs. 10 a-e. In places where data were lacking for a more accurate determination the curves have been filled out by means of an assumed hardening mechanism.

The age-hardening tests were conducted at 400, 500, 600, 700 and 500°C over times of 480 h. Maximum hardness values are attained at 600°C. The maximum hardness

is shifted towards shorter aging times for increasing Ti contents. A reduction in temperature at 400°C results in agehardening effects after protracted aging times only in the alloys with a fairly high titanium content. Increasing the temperature to 700°C causes hardening only in the alloys with a low Ti content; in the case of the alloys with the higher titanium content it immediately causes overaging.

The influence of silicon additions (1 and 1.5 %) on the age-hardening behavior of the V-3Ti alloy, containing about 1000 ppm oxygen, was investigated at 400, 500, 550 and 700°C (Figs. 11a,b). As can be seen from the diagrams, the addition of silicon in the homogenized state causes an increase in hardness of 40 and 70 kp/mm² respectively compared with the V-3Ti alloy. The addition of silicon accelerates the age-hardening behavior of the V-3Ti alloy. Maximum hardness values of 210 and 250 kp/mm² in alloys V-3Ti-1Si and V-3Ti-1.5Si respectively were achieved after heat treatment at 550°C for 72 h or 500°C for 360 h.

The influence of different boron and carbon contents on the age-hardening behavior of alloy V-3Ti with oxygen contents of around 600 ppm and nitrogen contents of 200 ppm was investigated at 450, 600, 750 and 900°C (Figs. 12a-c). If the boron content is raised to 750 ppm and the carbon content reduced to 120 ppm, the familiar age-hardening phenomena continue, but the peak hardness is recorded after shorter annealing times (Fig. 12a). If the carbon content is raised to 900 ppm and the boron content reduced to 4 ppm, no age hardening occurs (Fig. 12b). Slight age-hardening phenomena are observed again if the boron content is raised to 350 ppm (Fig. 12c).

The age-hardening tests on the V-2Zr alloys with oxygen contents of around 550 ppm and nitrogen contents of 200 ppm with different boron and carbon additions showed no age-hardening phenomena at temperatures of 250, 450, 600, 750 and 900°C (Fig. 13a-c).

1 1 1 1 1

Noticeable age hardening was observed on the alloy V-IIIf with oxygen and nitrogen contents of around 500 and 150 ppm respectively with different boron and carbon additions at an aging temperature of 250°C (Fig. 13d,e). A V-IHf alloy to which 5 ppm boron and 1050 ppm carbon had been added reached a hardness of 160 kp/mm² after an aging time of 120 h at 250°C, which corresponds to an increase in hardness of 60 kp/mm² compared with the homogenized state. At the same aging temperature, annealing for

3 h produces an increase in hardness of 70 kp/mm² in a V-1Hf alloy containing 400 ppm boron and 1000 ppm carbon. Age-hardening tests at 450, 600, 750 and 900°C resulted generally speaking in a reduction in hardness compared with the values for the homogenized states.

4.2 Tensile Fests

Tensile tests were conducted on the alloy V-1Ti at room temperature and at 350°C.

The samples of the alloy were in the homogenized state, as well as samples which had also been aged at 600°C/20 d, 700°C/3 d and 700°C/20 d. The samples of the homogenized state showed a rise in the tensile strength and yield point with temperature. The elongation on rupture was the same (15 %).

The highest tensile strength values at room temperature (83 kp/mm²) were reached

by aging at 600°C for 20 d. The elongation on rupture values for the samples aged as above were about 10 % for both test temperatures (Fig. 14).

High tensile strength values were not obtained with the V-3Ti alloys containing carbon, boron + carbon and the V-2Zr alloys containing boron, which were aged for 24 h at 600°C (Fig. 15). The strength values are below 50 kp/mm². A strength of slightly above 50 kp/mm² at room temperature was recorded for a V-3Ti-1Si sample aged at 700°C for 7 h. The elongation on rupture values for these alloys were between 10 and 16 % at room temperature and at 350°C, with necking values between 45 and 70 % (Fig. 16).

The highest necking values on rupture were attained for alloy V-3Ti-1Si. There is a general tendency for these to increase with rising temperature.

A surprising feature is the occurrence of a marked yield point at the two test temperatures both for the V-3Ti-1Si alloy aged at 700°C for 6 h (Fig. 17) and for the V-3Ti alloy containing boron or carbon additions aged at 600°C for 1 day (Figs. 18 and 19). No pronounced yield point is observed in V-3Ti alloys containing boron and carbon (Figs. 18 and 19).

Only tensile tests at room temperature were carried out on the V-lHf alloys; the corresponding stress/strain diagrams show no marked yield points. Table 3 shows the tensile strength, elongation and necking values for homogenized tensile specimens and also for tensile specimens of alloy

V-llif containing carbon and carbon + boron which had been aged at 250°C for 45 min. The maximum strength value of 60.5 kp/mm is recorded for the V-llif alloy with boron and carbon additions which was aged at 250°C for 45 min; this amounts to an increase in strength of about 65% compared with the homogenized state. The elongation on rupture drops merely from a value of 16% to 11%, but the necking falls from 77.8% to 46.2%.

4.3 Metallographic Examination

The micrographs of the homogenized conditions of the alloys V-1Ti and V-20Ti show that increasing Ti contents are accompanied by a pronounced coarsening of the particles which have already been precipitated (Figs. 20a, b). For increasing aging temperature and time the primarily precipitated particles are coarsened. In addition, strong precipitates are observed at the grain boundaries and sub-grain boundaries which, as can be shown on a V-3Ti alloy aged at 600°C for 10 d and on a V-20-Ti alloy aged at 700°C for 10 d (Figs. 21a,b), are so close together that needle-shaped precipitates can be simulated in the matrix as a result of the surface etching. The matrix also contains finely divided precipitates which form precipitation structures, mainly after long-time annealing at low temperature, but with uniform grain boundary edges (Fig. 21c).

V-3Ti alloys with varied carbon and boron contents which were aged at 600°C for 24 h display no discrepancies compared with the micrographs shown hitherto; the same holds for the V-3Ti alloys containing 1 and 1.5 % Si. The C-containing specimens of the V-2Zr alloys containing different

boron and carbon contents and aged for 24 h at 600°C show finely dispersed precipitates at the sub-grain boundaries (Fig. 22). The samples also contain pronounced precipitates at the grain boundaries. The micrographs of the V-Hf alloys reveal no new phenomena in the homogenized or in the aged state, compared with the vanadium alloys containing titanium.

5. Discussion of Results

If the results described above are considered with respect to their technical application, the following conclusions can be drawn:

The tensile strength of low-alloy vanadiumbase alloys can be raised considerably at toom temperature and slightly elevated temperatures through the precipitation hardening of the TiO phase. By the addition of favorable solid solution hardeners, optimum composition of the interstitial additions and treatment before and after precipitation hardening, it will certainly be possible to raise the tensile strength of low-alloy vanadium-base alloys to

100 kp/mm² while retaining several percent elongation. If consideration is given to the ratio between the tensile strength aimed at and the specific weight of the low-alloy vanadium alloys compared with the corresponding values for normal alloys, e.g., Udimet 600 or Ti-GA1-4V (Fig. 23), the values of the vanadium alloys are well below those of other alloys. Fig. 23 shows the ratio of the tensile strength to the specific weight of the V-lTi alloy investigated here.

The exploitation of the age-hardening processes

in vanadium alloys in order to increase the creep resistance is restricted to temperatures of less than 750°C, since overaging occurs after a short time above this temperature.

The conclusion to be drawn with respect to the extrusion of V-Ti alloys is that the temperature during extrusion should not drop below 800°C unless greater resistance to deformation is acceptable or unless, by reducing the oxygen content or increasing the carbon, precipitation-hardening processes are not required during the subsequent use of the alloy.

The investigations described here throw some new light on the scientific understanding of the behavior of vanadium-base alloys.

The hardening of V-Ti and V-Ti-Si alloys is certainly produced by the precipitation of the TiO phase, as was demonstrated by K.H. Kramer (Ref. 6). It should be borne in mind here that even in the homogenized state a large number of primarily precipitated particles are present which tend to become coarser for increasing Ti contents. a result of aging, secondary TiO is then precipitated, leading to a considerable increase in hardness. The supposition that the increase in hardness is due to the uptake of oxygen or nitrogen during annealing has been disproved by the chemical analysis of the aged samples.

No knowledge has emerged concerning the mechanism by which boron does not exert a negative influence on the age-hardening behavior of the V-Ti-O alloys, while carbon

permits only slight increases in hardness, the addition of boron to carbon-containing V-Ti-O alloys in turn causing age hardening. Investigations aimed at clarifying these phenomena will doubtless have to be based on the mutual influence of the mobility of the elements B, C and O. Because they occupy interstitial sites, the carbon atoms will influence the mobility of the oxygen and impair the homogeneous nucleation of the TiO phase rendered possible by thermal concentration fluctuations.

If it is assumed that boron is dissolved substitutionally in the vanadium lattice, which is probable, since boron has a 15 % greater atomic radius than that of the largest vacancy in vanadium, the lattice constant is reduced by the addition of boron, since the atomic radius of boron is smaller than that of vanadium. reduction in the lattice constant has a greater effect on the mobility of the larger carbon atoms than on that of the somewhat smaller oxygen atoms. In the presence of carbon, the addition of boron therefore has the effect of reducing the carbon content. Slight age-hardening phenomena can therefore appear, and are in fact observed.

It is also interesting that marked yield points occur in the V-3Ti alloys containing carbon which were not demonstrated in a work by H. Böhm and F. Mir (Ref. 7). These authors only found marked yield points above a Ti content of over 5 %. The occurrence of a marked yield point for higher Ti contents is attributed by K.H. Kramer (Ref. 6) to the fact that for increasing Ti content the lattice constant of the V-Ti alloys increases, as a result of which the ratio of the dissolved to the precipitated oxygen increases for rising titanium contents

and the blockage of the dislocations is enhanced. However, the studies conducted by these authors indicate that the carbon has a greater influence on the occurrence of a marked yield point.

If a marked yield point occurs in V-Ti alloys, this will also have to do with the aging condition as well as the chemical composition, i.e., the more oxygen is withdrawn from the system by TiO precipitation, the earlier carbon can start to act to produce the Lüders lines. Additions of silicon, which accelerates age hardening in V-Ti alloys, intensify the marked yield point and the Portevin-LeChatelier effect.

The fact that V-Ti alloys containing 3 % Ti show optimum long-term creep rupture behavior, as demonstrated by H. Böhm and M. Schirra (Ref. &), can be regarded as due to the overlapping effect of solid solution hardening, precipitation hardening and accelerated overaging for increasing titanium contents.

The influence of nitrogen on the age-hardening behavior and on the formation of the marked yield point has so far not been discussed. Special studies should be conducted in order to determine whether and to what extent nitrogen has an influence on the abovementioned phenomenon.

Studies on the orecipitation behavior of nitrogen in vanadium have been carried out by D. Potter and C. Altstetter (Ref. 9). In a vanadium samples containing 3 a/o nitrogen which had been annealed at 350°C for 47 h, these authors demonstrated a superlattice structure in accordance with the stoichiometric composition V_{16}^{N} .

The work of D. Potter and C. Altstetter (Ref. 9) also points out the tendency of the body-centered cubic metals V, Nb and Ta to arrange the interstitial elements N, O and C in clusters. At higher concentrations the interstitial elements form superlattice structures with the metals in the VA group, as has already been shown for the systems Ta-C, Ta-N, Ta-O, Nb-O and V-O.

No further studies have been performed on the precipitation behavior of the V-Zr alloy or on the clarification of the precipitation hardening of the V-lHf alloy.

6. Abstract

An investigation was performed to determine the influence of N, C, B and C on the precipitation and age-hardening behavior of the alloys V-Ti, V-3Ti-Si and V-2Zr V-1Hf.

The alloys V-Ti-O and V-Hf-C were found to be precipitation-hardening systems. In the system V-Ti-O it is the semi-coherent precipitation of TiO which causes hardening, while in the system V-Hf the phase responsible for hardening still has to be determined.

The addition of boron or silicon speeds up hardening in the alloy V-Ti-O, while carbon impairs it.

Carbon plays an important part in the occurrence of a marked yield point in V-Ti-O alloys. The appearance of marked yield points is enhanced by increasing the carbon content and by annealing in the hardening range.

It is not at present possible to indicate new fields of application for vanadium-base alloys outside that of nuclear engineering.

7. Literatur

- R. Kieffer, H. Braun
 "Vanadin, Niob, Tantal" 1963
- 2) H. Beißwenger, H, Blank
 "Die Entwicklung von Brennelementen Schneller Brutreaktoren", KFK 700, 1967
- 3) D.R. Matthews, G.H. Keith, E.A. Loria Bu Mines Rept. of Inv. 6637, 1965, 23pp
- 4) T.C. Holtz, L.B. Richard

 JJTRJ-B 6007-6, 1964, Final-Report
- 5) H.G. Werson, D.R. Matthews, J.S. Winston Rep. Invest. No. 7113, U.S. Dept. of the Interior, 1968
- 6) K.-H. Kramer

 Journal of the Less-Common Metals, 21,(1970) 365-382
- 7) H. Böhm, F. Mir KFK-524, 1966
- 8) H. Böhm, M. Schirra KFK-774, 1968
- 9) D. Potter, C. Altstetter
 Acta Metallurgica, 1971, Vol. 19, No. 9, S. 881-886
- 10) B.R. Rayaler u. R. J. van Thyne
 J. Less.-Common Metals, 1961, S. 489

Löslichkeitsgrenzen einiger Elemente in Vanadin bei höheren Temperaturen und mögliche binäre Phasen bei tieferen Temperaturen.

Tabelle 1

Element	max.Löslichkeit in Gew%	Temperatur ^O C	Phase	Struktur	Gitterkonstante
Zr	5	600	ZrV ₂	hex.	a = 5,288; c = 8,664
Hf	1,2	1200	HfV_2	kub. MgCu	a = 7,386
Fe	37	600	FeV	hex. CrFe	a = 8,95; c = 4,62
Co	8	600	V ₃ Co	kub. β-W	a = 4,675
Ni	8	600	V ₃ Ni	kub. β-W	a = 4,71
ΑI	26	600	V ₅ Al ₈	kub.	a = 9,207
Si	3	1200	V ₃ Si	kub. β-W	a = 4,721
Sn	20	600	V ₃ Sn	kub. β-W	a = 4,91
Be	0,8	900	Be ₂ V	hex.	a = 4,394; c = 7,144

Tabelle 2

Gehalt der interstitiellen Beimengungen N, O, B und C

LegNr.	Legierung	N (ppm)	O (ppm)	B (ppm)	C (ppm)
1	V-1Ti	260	850	-	820
2	V-3T i	390	1200	-	610
3	V-5T i	400	520	-	470
4	V-10Ti	370	540	-	430
5	V-20T i	310	460	-	360
6	V-3Ti-1Si	250	950	-	650
7	V-3Ti-1,5Si	365	1000	-	410
8	V-3Ti	300	500-690	750	120
9	V-3Ti	180	530-600	4	900
10	V-3Ti	145	550-770	350	915
11	V-2Zr	240	500-640	900	120
12	V-2Zr	165	500-610	4	920
13	V-2Zr	165	490-600	400	880
14	V-1Hf	170	490-580	5	1050
15	V-1Hf	135	470-520	400	1000

Tabelle 3

Mechanische Eigenschaften der Legierung V-1Hf

Legierung	Zustand	Festigkeit (kp/mm ²)	Streckgrenze (kp/mm²)	Bruchdehnung (%)	Brucheinschg. (%)
V-1Hf+B,C	homog.: (1250 ⁰ C, 1h/W)	36,6	27,7	16,4	77,8
11	homog. + 250°C,45'	60,5	51,3	11,0	46,2
V-1Hf+C	homog.: (1250 ⁰ C, 1h/W)	33,5	23,4	17,5	83,2
	homog.+ 250°C,45'	55,3	47,6	10,5	58,7

 $T = 25^{\circ}C$, $\epsilon = 2.4 \cdot 10^{-4} (^{1}/\text{sec})$

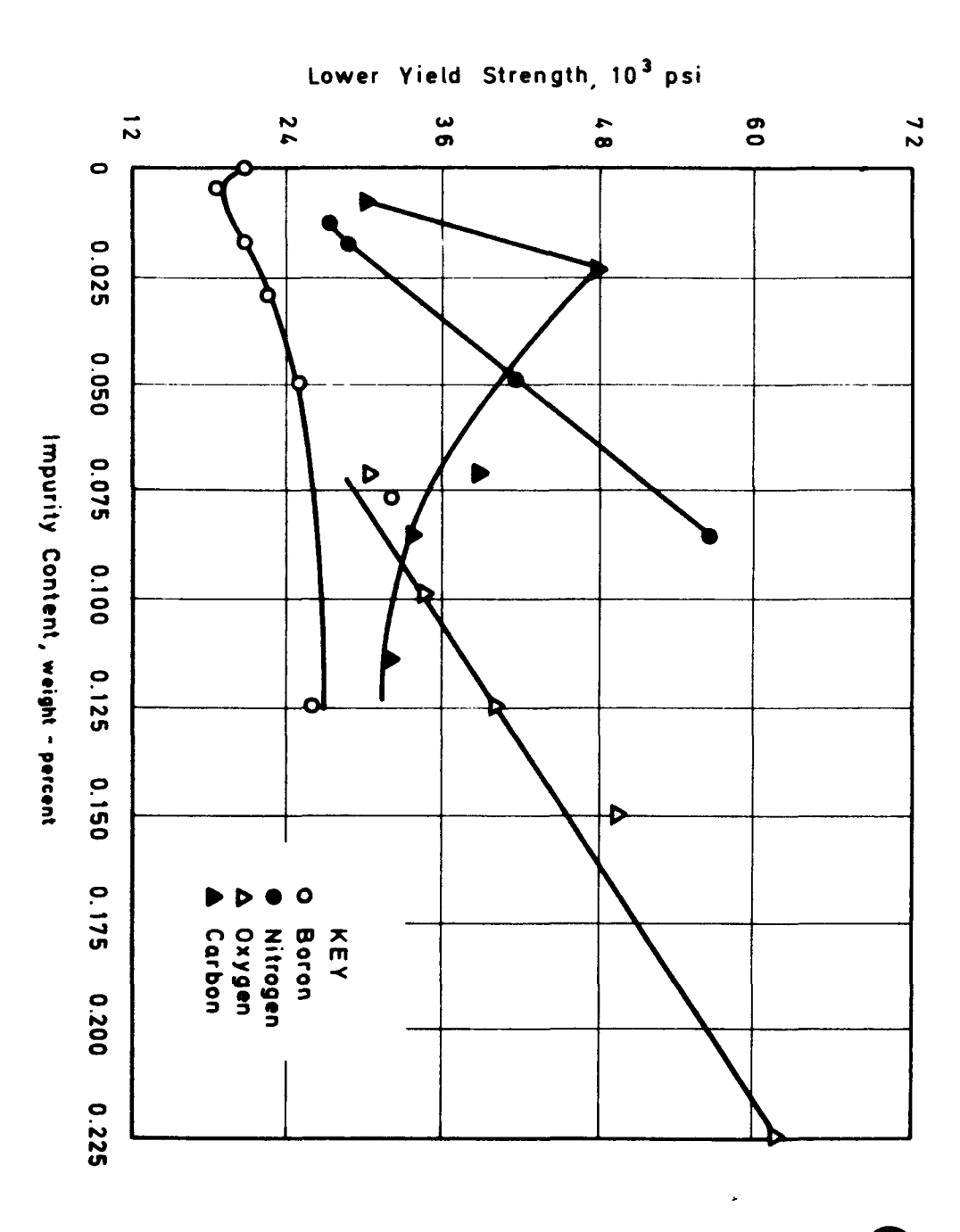


Bild Der Einfluß von interstitiellen Verunreinigungen auf die Streck-grenze von Vanadium bei einer Temperatur von 273 °k 3)

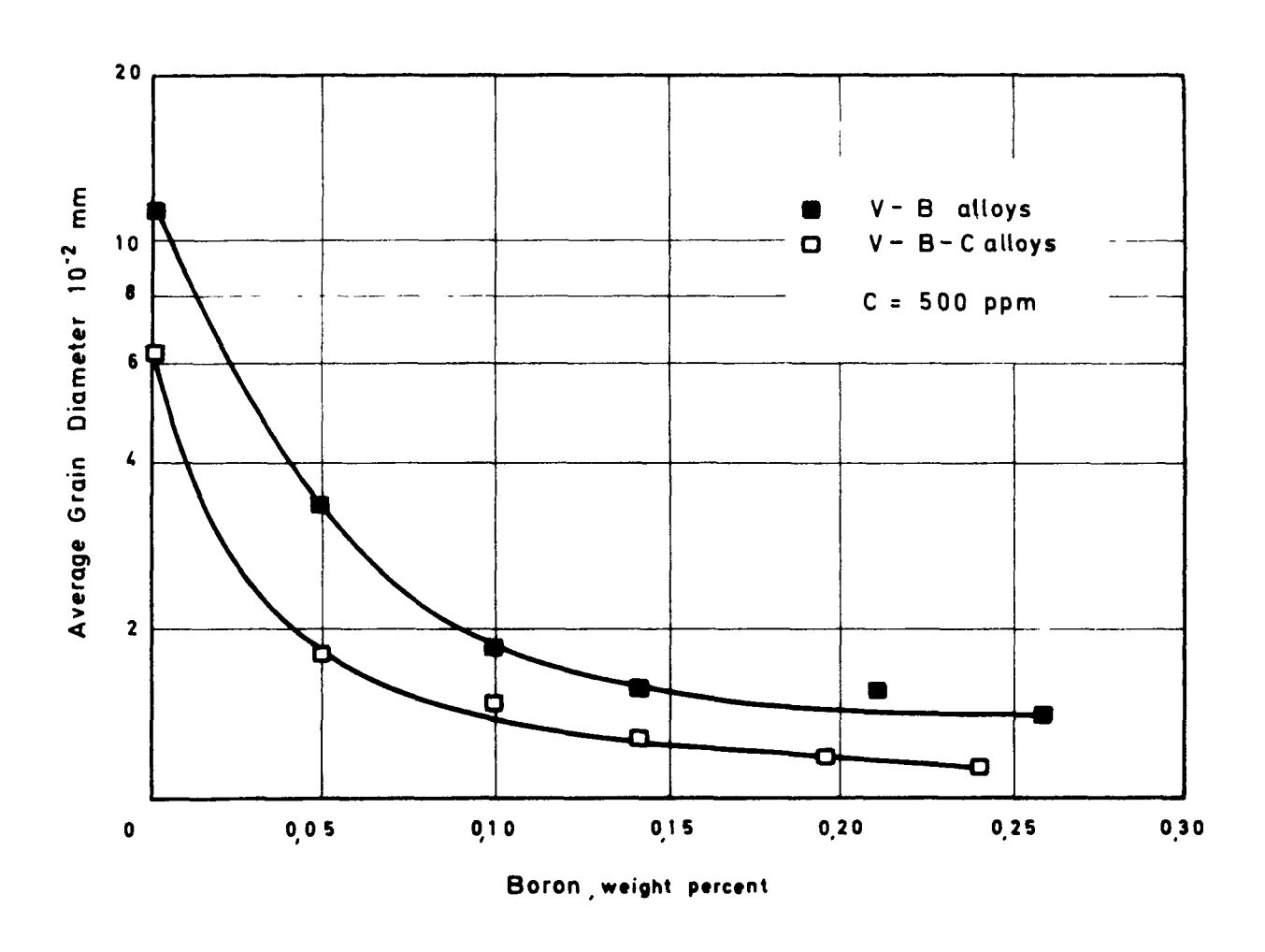


Bild 2: Durchschnittlicher Korndurchmesser nach 90 % iger Verformung und anschließender Rekristallisation ($T_R = 800 - 1100$ °C; $t_R = 5 - 150$ min)

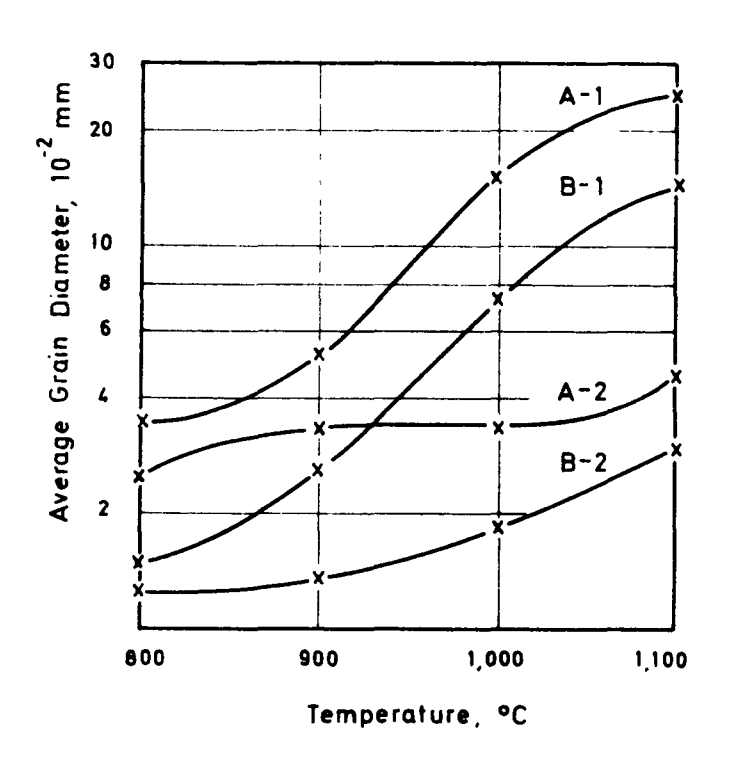


Bild 3: Durchschnittlicher Korndurchmesser nach 90 % iger Verformung und anschließender Rekristallisation in Abhängigkeit von der Rekristallisationstemperatur. 5)

	B (ppm)	C(ppm)	0(ppm)	N(ppm)
A-1	-	180	49	40
A-2	480	170	41	10
B-1		520	45	20
B 2	470	550	_	20

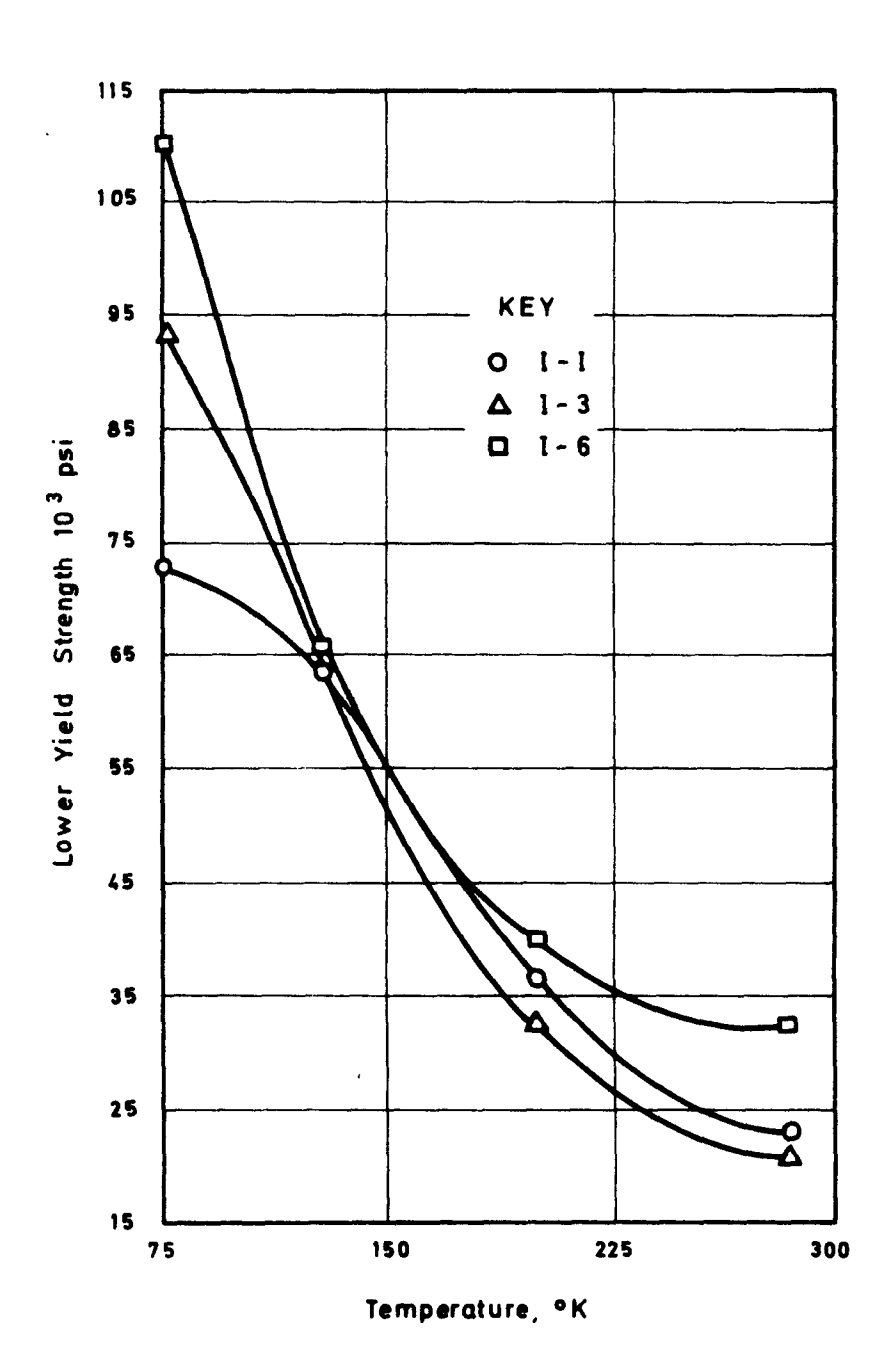


Bild 4: Temperaturabhängigkeit der Streck – grenze bei Vanadium und Vanadium – Bor – Legierungen 5)

	B (ppm)	C(ppm)	0 (ppm)	N (ppm)
I - I	-	95	3 4 5	35
1 - 3	180	60	430	25
I - 6	760	65	480	25

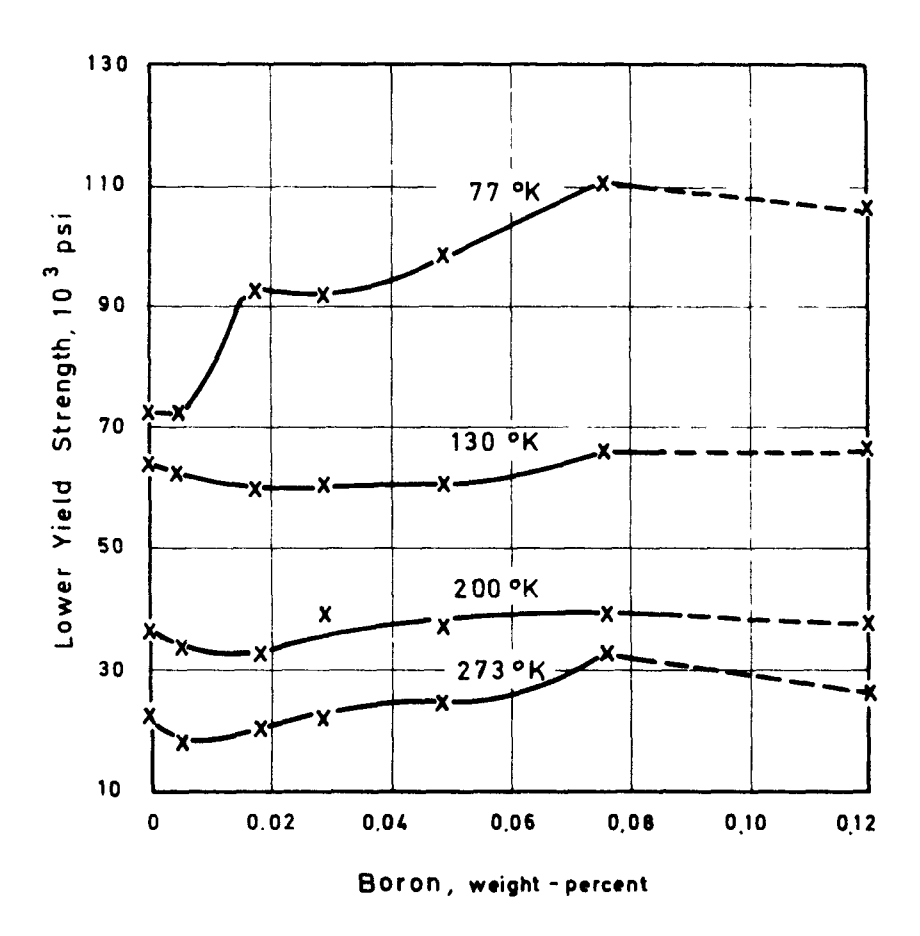


Bild 5: Einfluß des Borgehaltes auf die Streckgrenze von Vanadium bei verschiedenen Temperaturen ⁵⁾

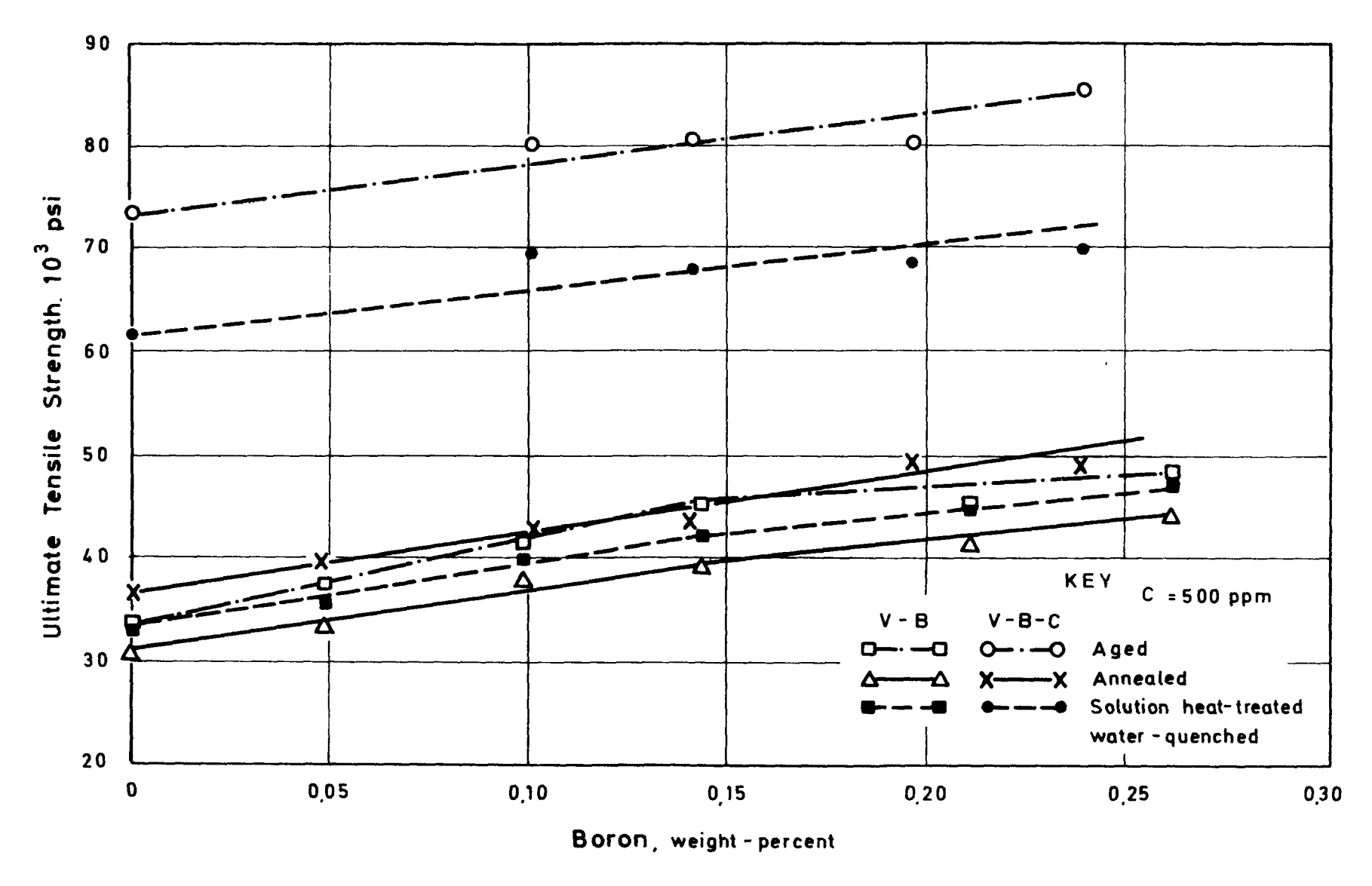


Bild 6: Einfluß von Bor und Bor + Kohlenstoff auf die Festigkeit von Vanadium bei 298 °k 5)

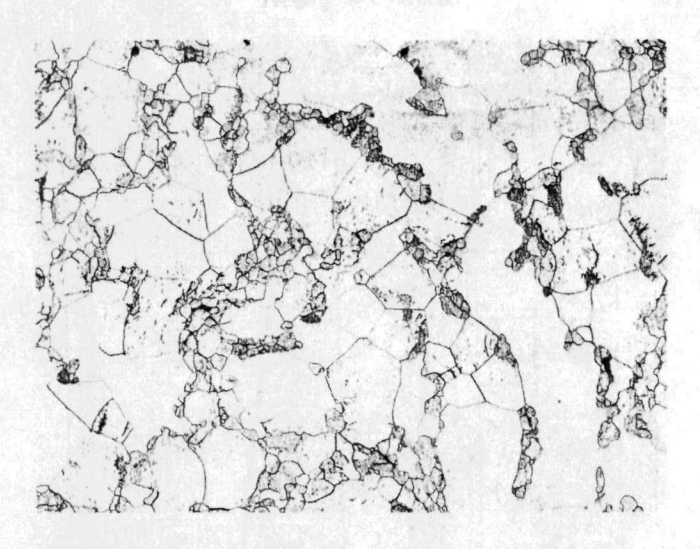


Bild 7a

Legierung: V-3Ti + 800 ppm C Zustand: homog. + 600°C, 1d





Bild 7b

Elektronenrasteraufnahme der Ti-Röntgenstrahlung

Legierung: V-3Ti

Zustand: homog. + 500°C, 20d



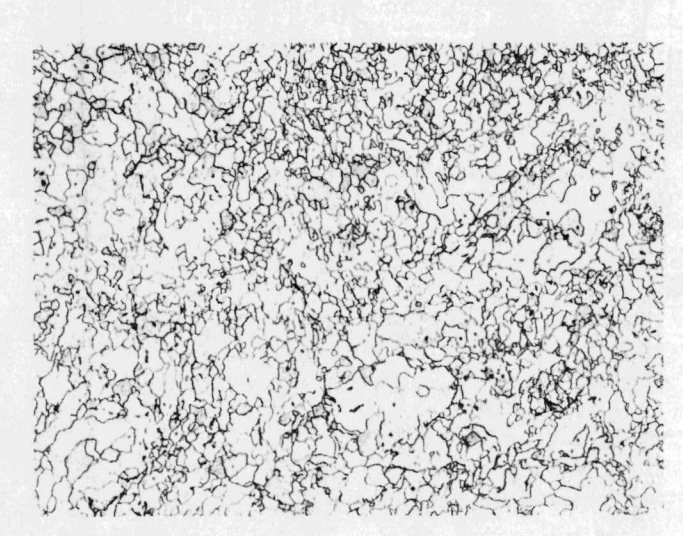
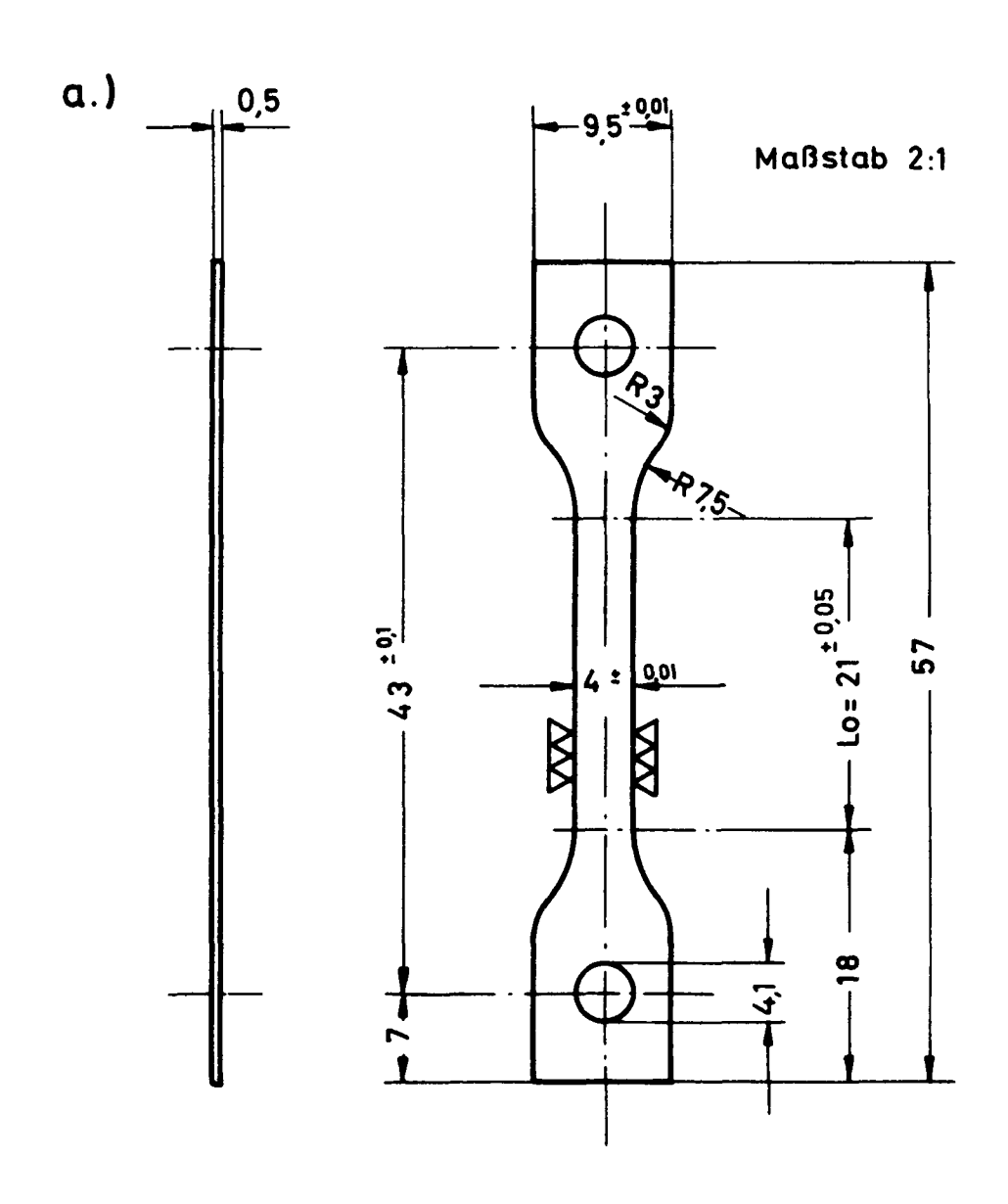


Bild 8

Legierung: V-1Hf + 800 ppm C + 400 ppm B

Zustand: homog. + 600°C, 1d



b.) Maßstab 2:1

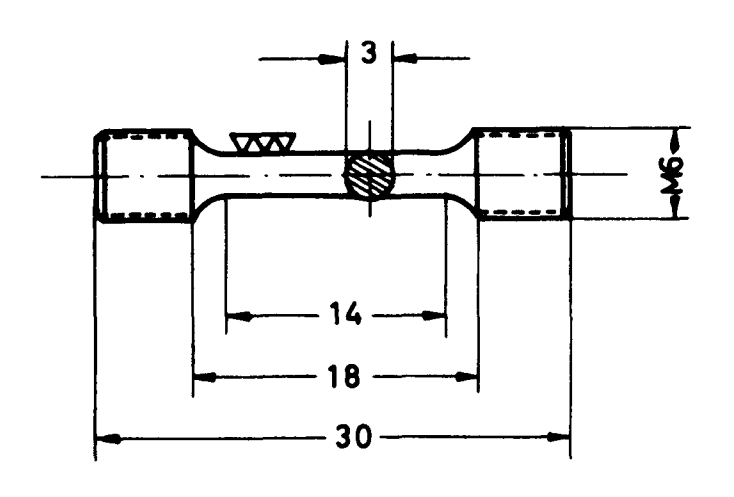


Bild 9a u.b.: Zugproben

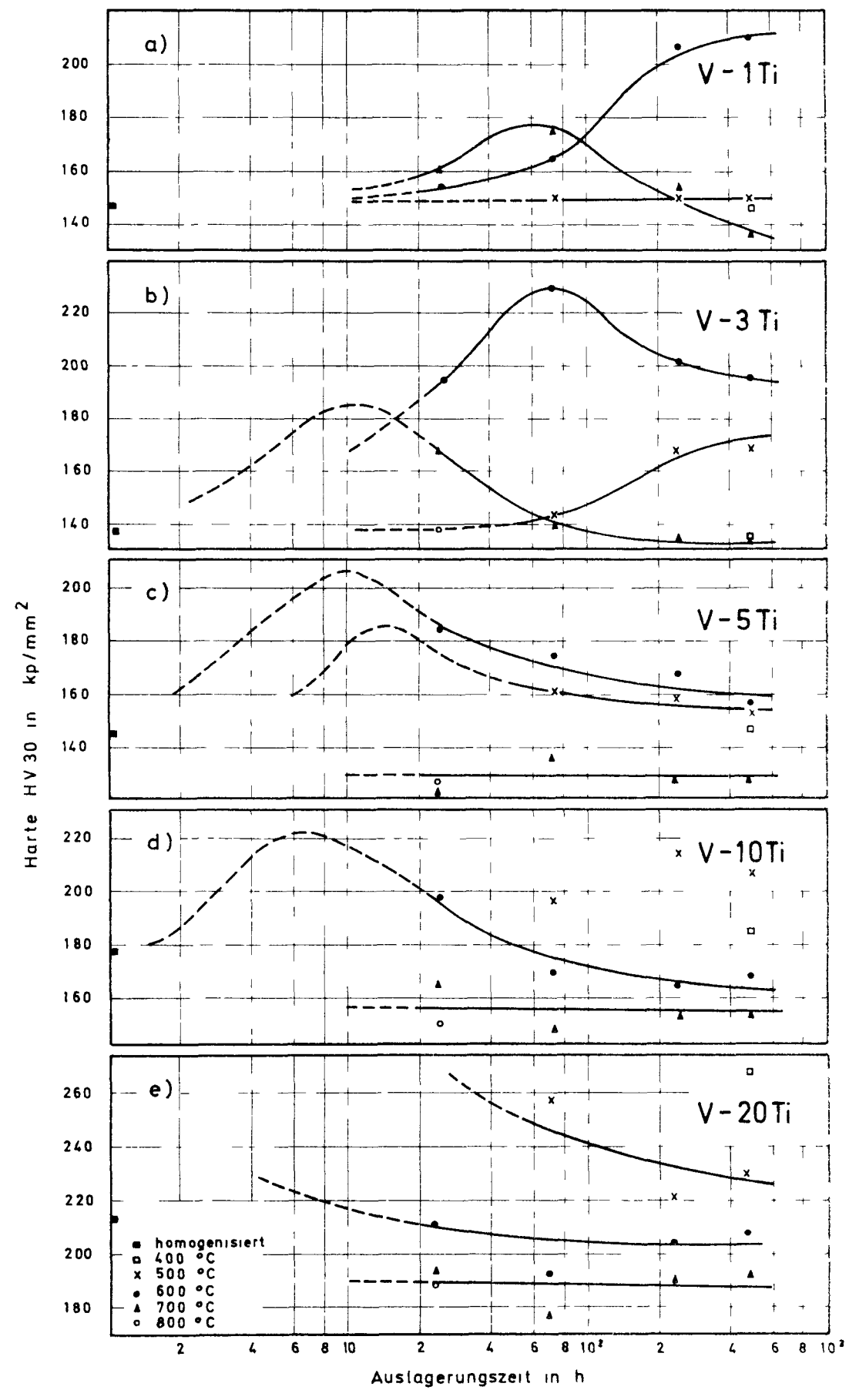


Bild 10a-e: Härteverlauf in Abhängigkeit von der Auslagerungszeit und der Auslagerungstemperatur

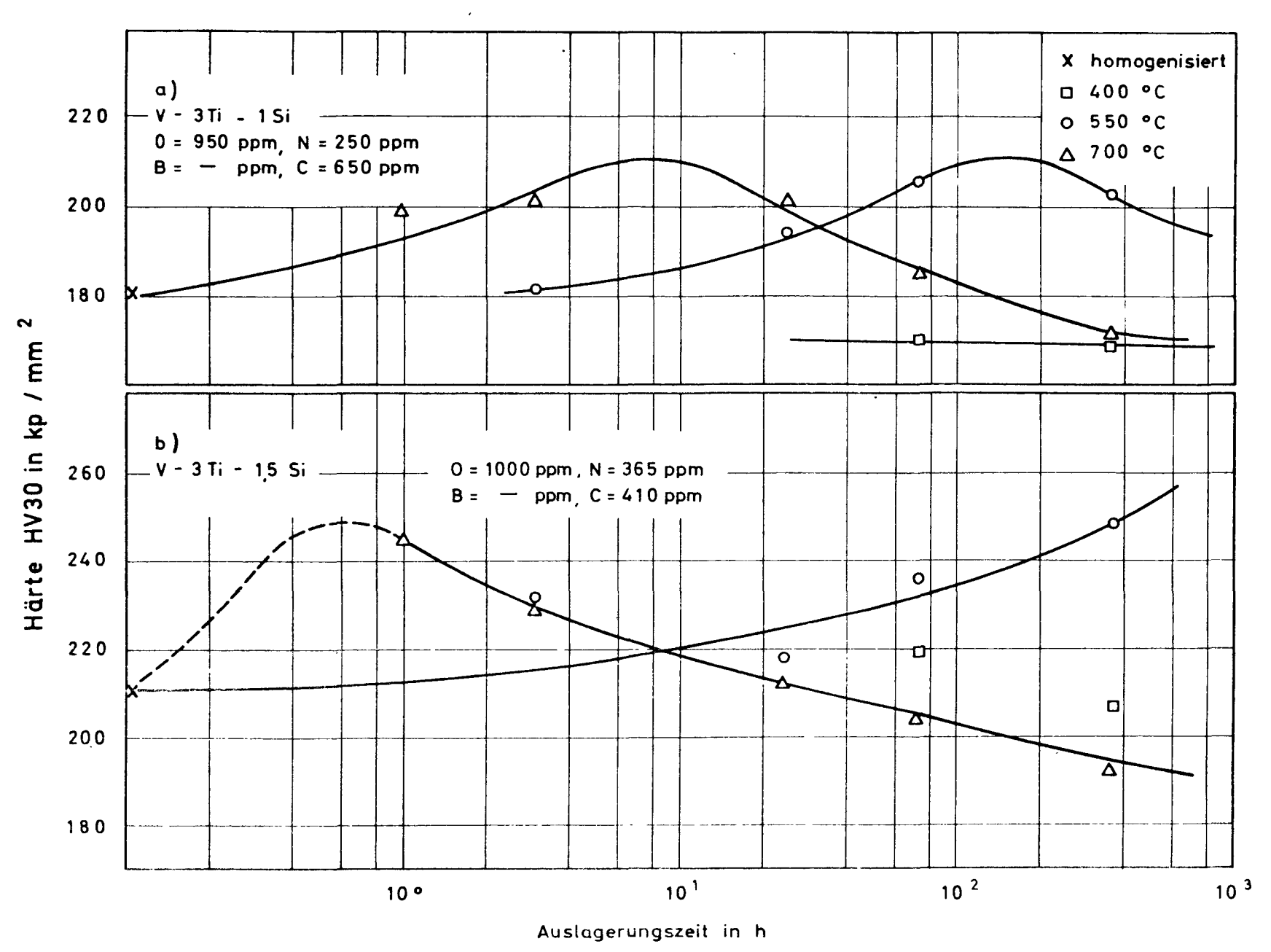


Bild 11 a u.b: Härteverlauf in Abhängigkeit von der Auslagerungszeit und

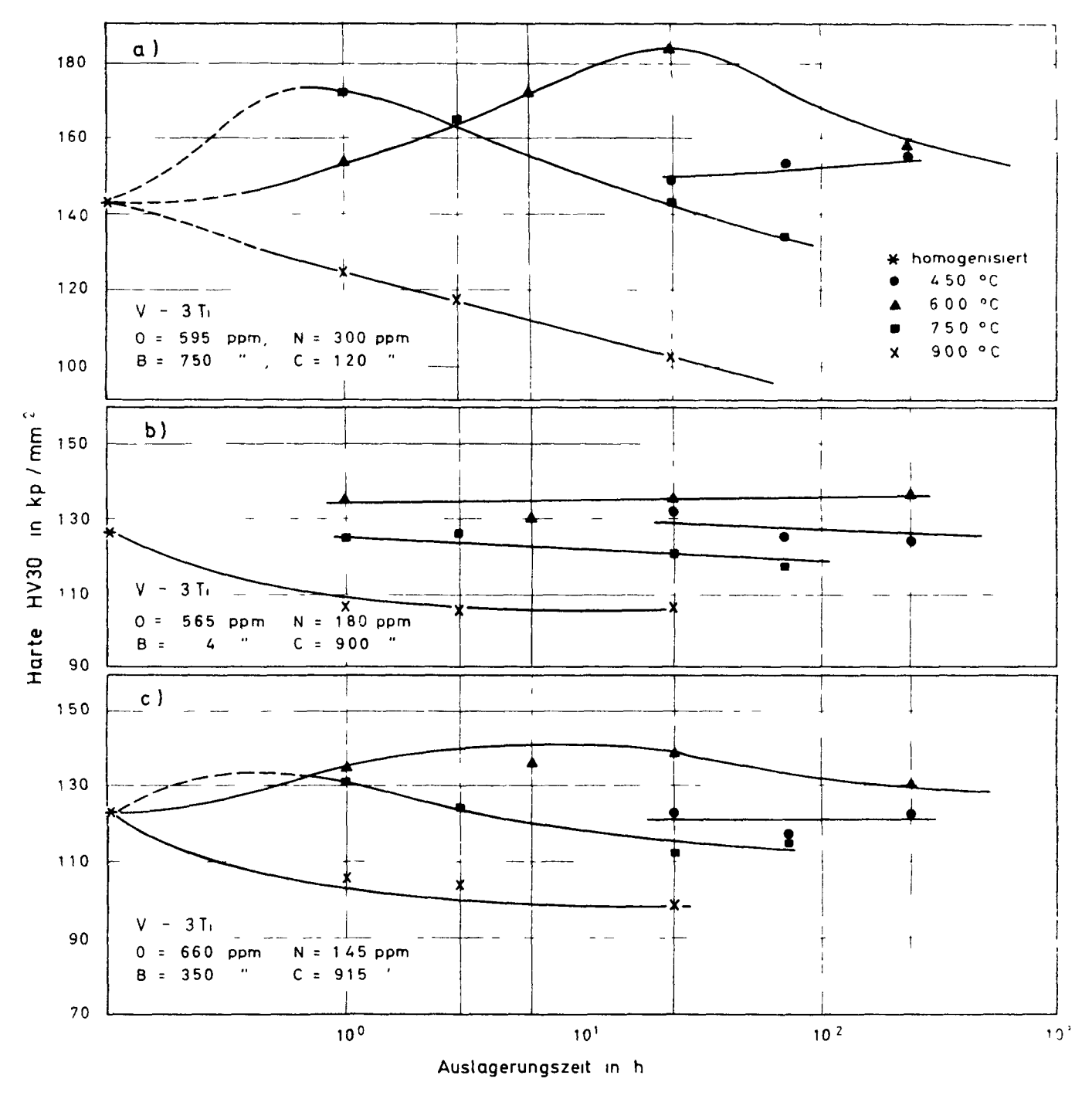


Bild 12a-c : Härteverlauf in Abhängigkeit von der Auslagerungszeit und der Auslagerungstemperatur

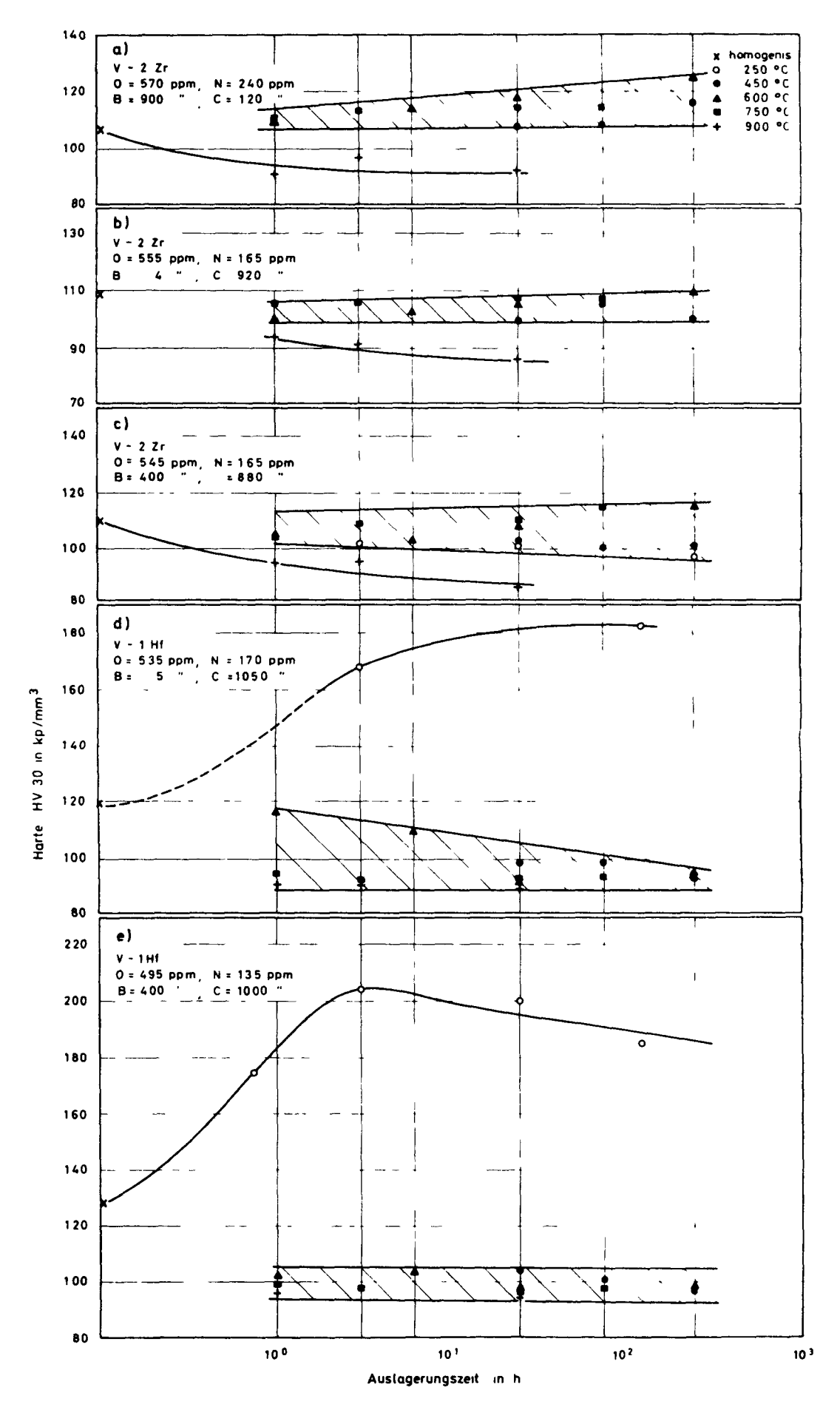


Bild 13a-e: Härteverlauf in Abhängigkeit von der Auslagerungszeit und der Auslagerungstemperatur

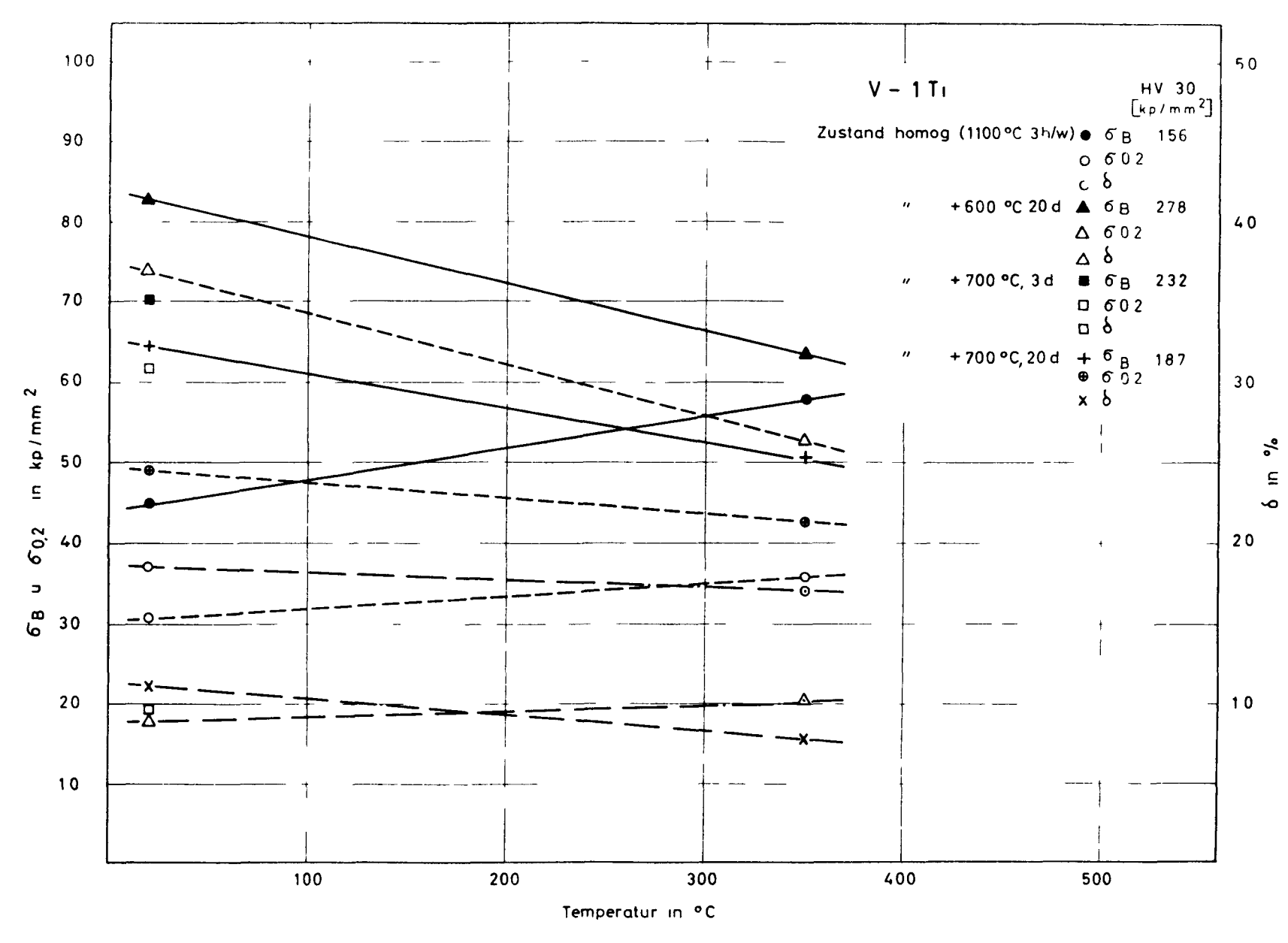


Bild 14: Zugfestigkeit, σ_B , Streckgrenze, $\sigma_{0,2}$ und Bruchdehnung, δ , in Abhängigkeit von der Temperatur

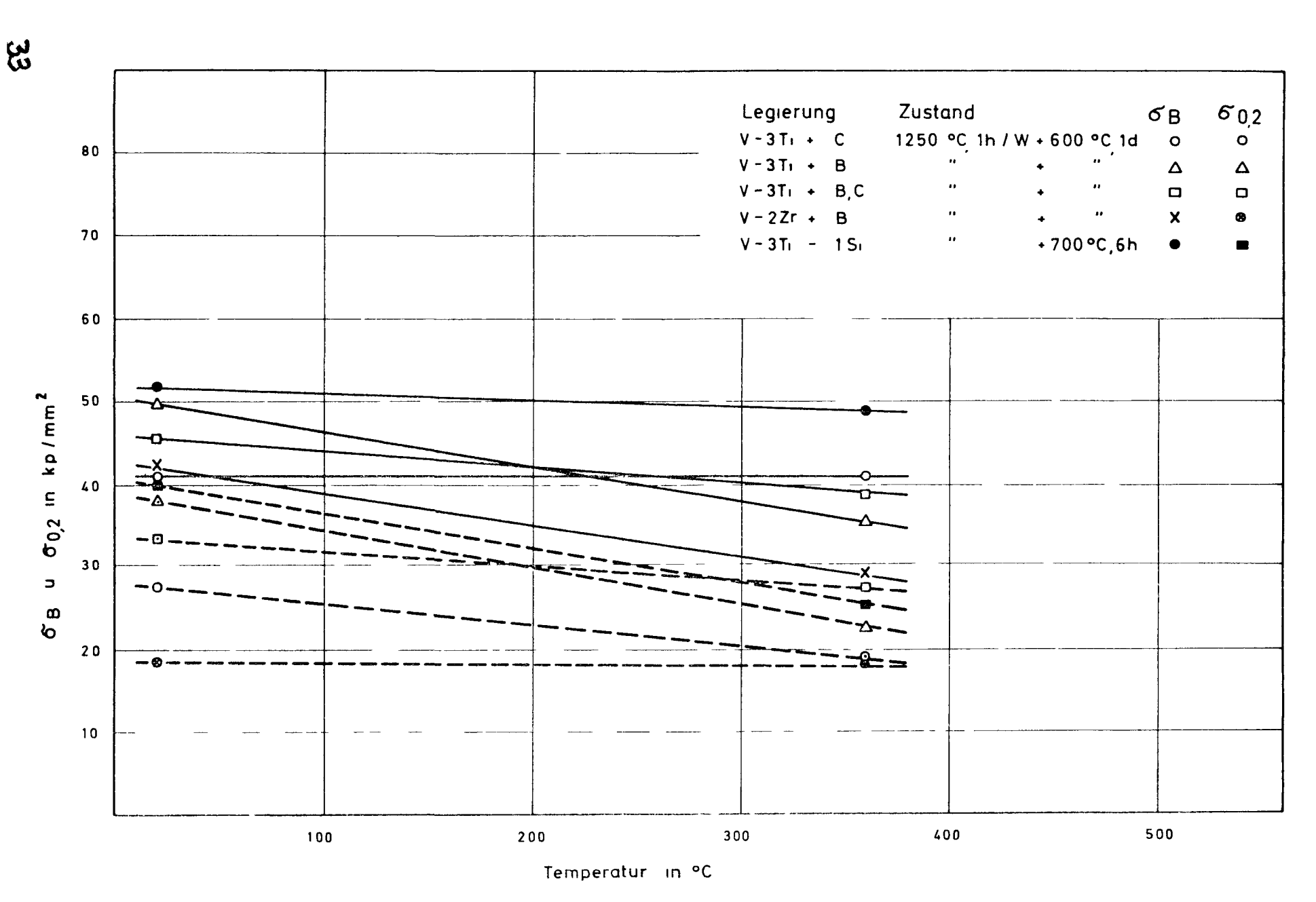


Bild 15. Zugfestigkeit, σ_B , Streckgrenze, $\sigma_{0,2}$, in Abhängigkeit von der Temperatur

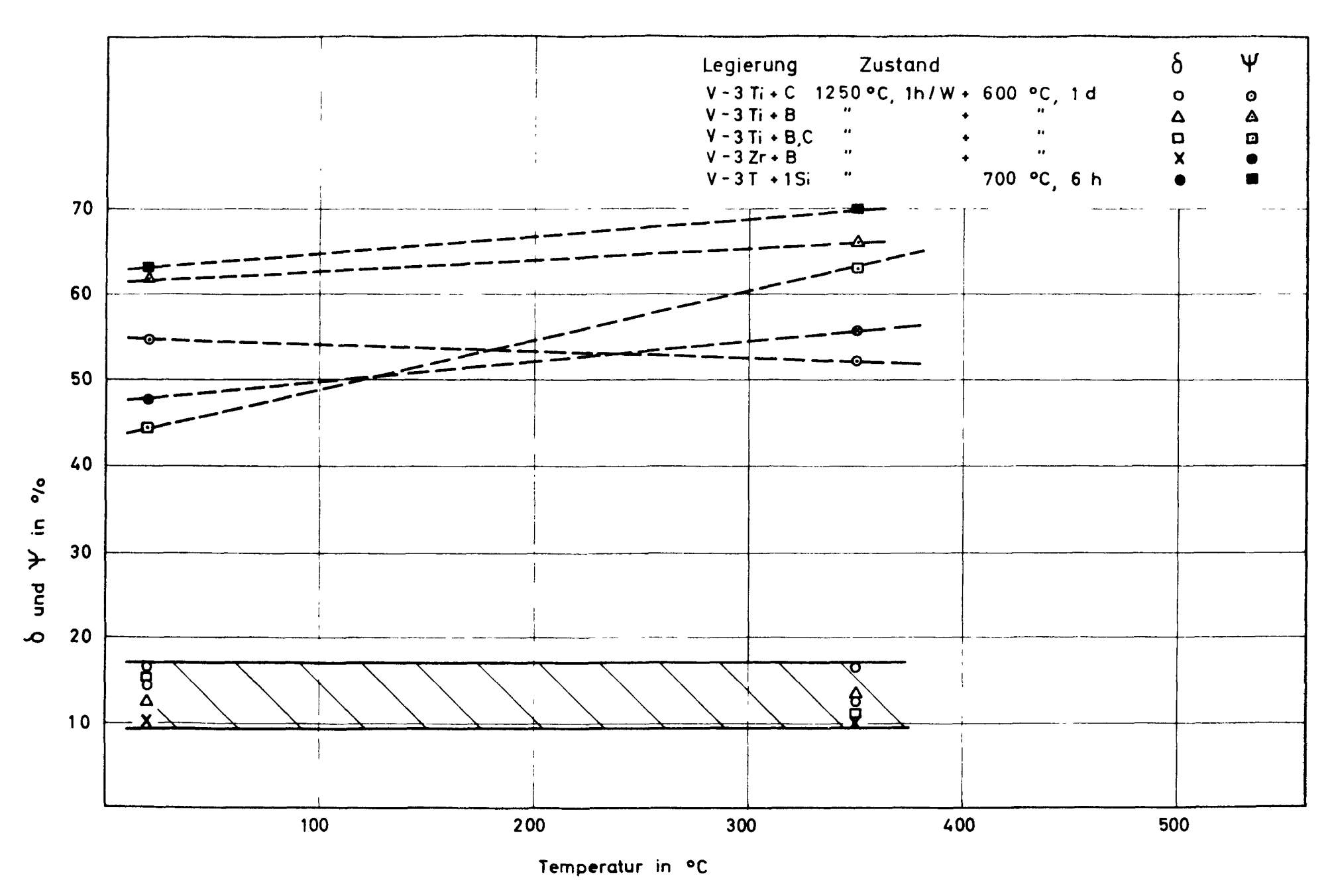


Bild 16: Bruchdehnung, d. Brucheinschnürung, Y. in Abhängigkeit von der Temperatur



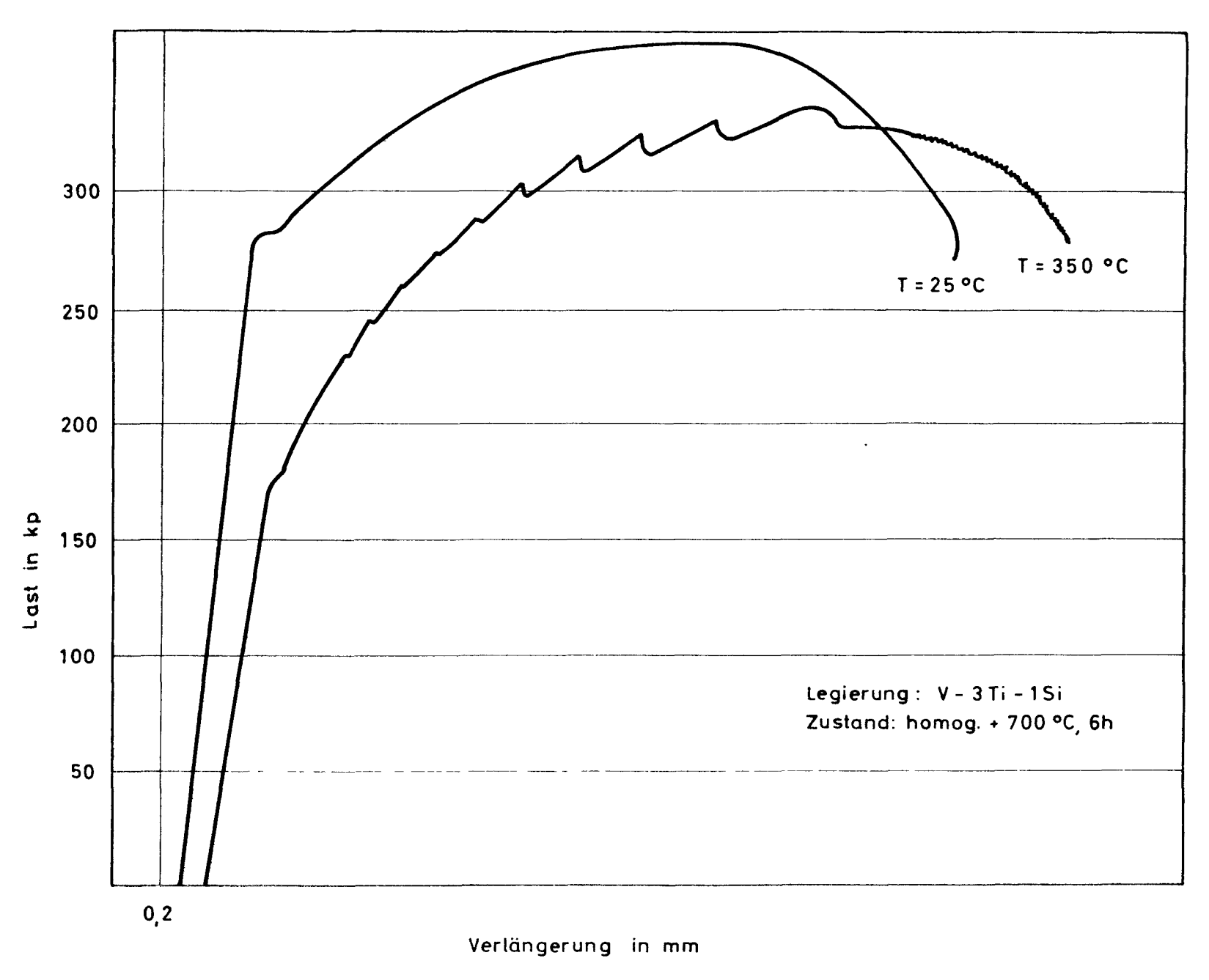


Bild 17: Last - Verlängerungsdiagramme bei verschiedenen Temperaturen

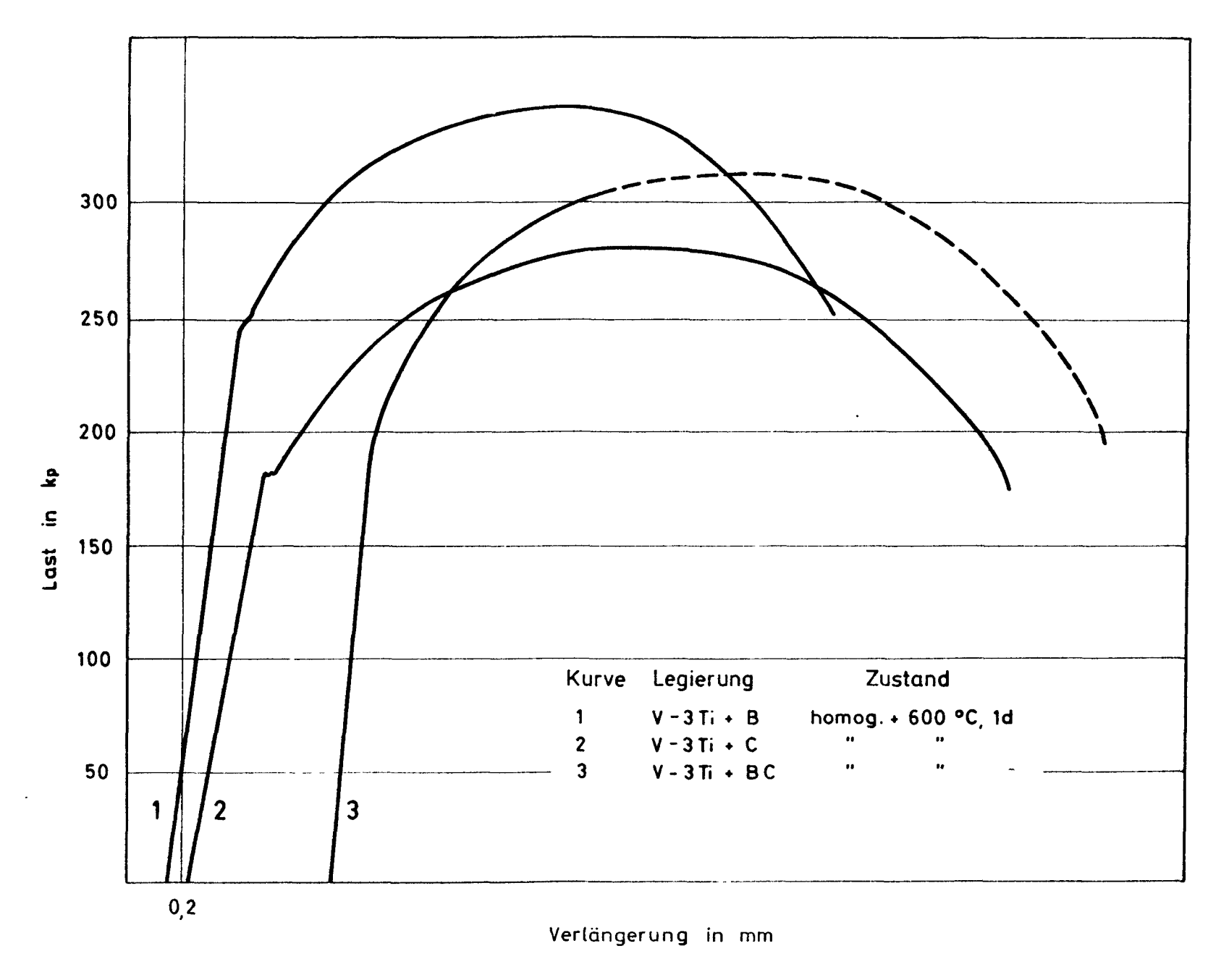


Bild 18: Last - Verlängerungsdiagramme bei Raumtemperatur

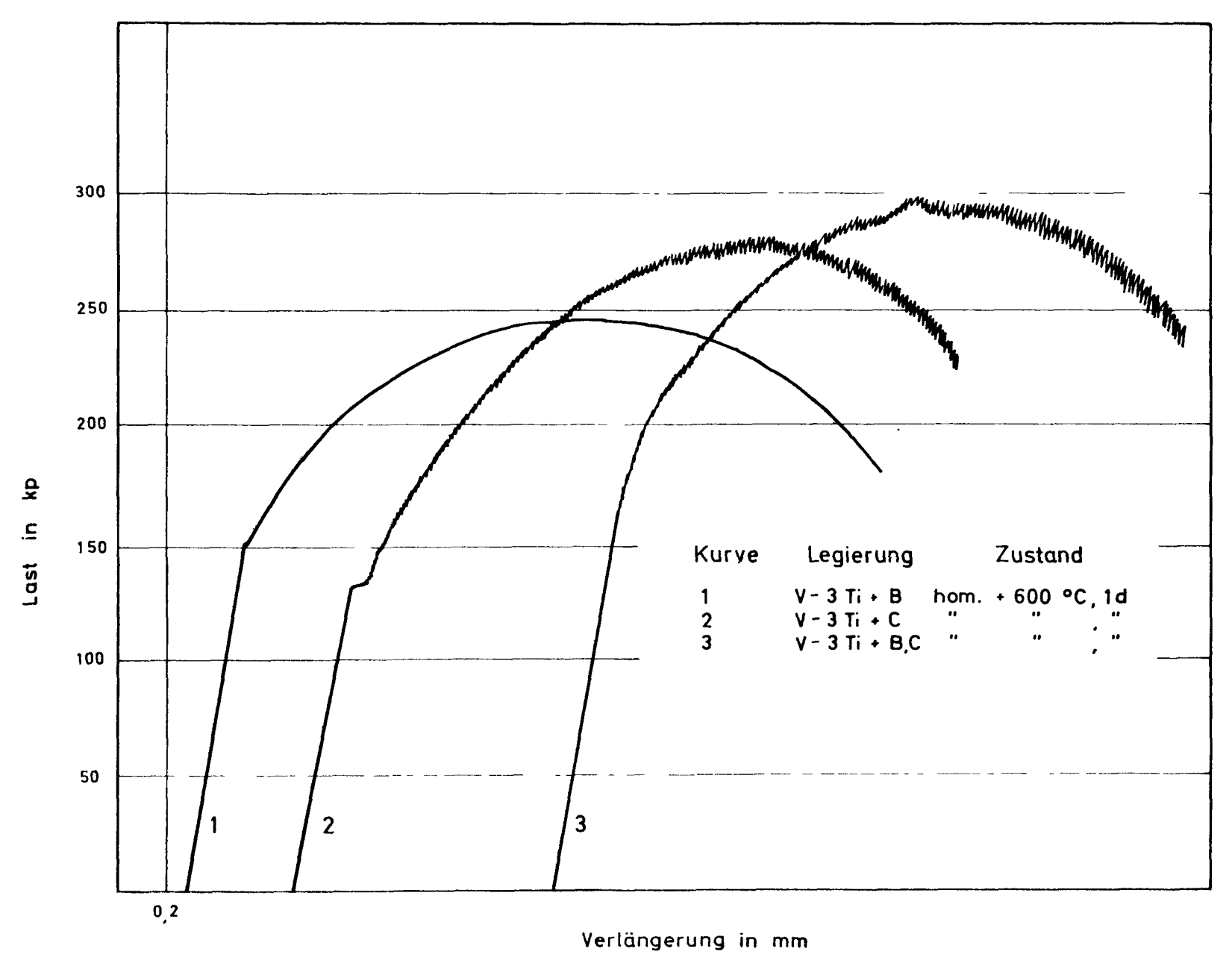


Bild 19: Last - Verlängerungsdiagramme bei 350 °C

 \subseteq

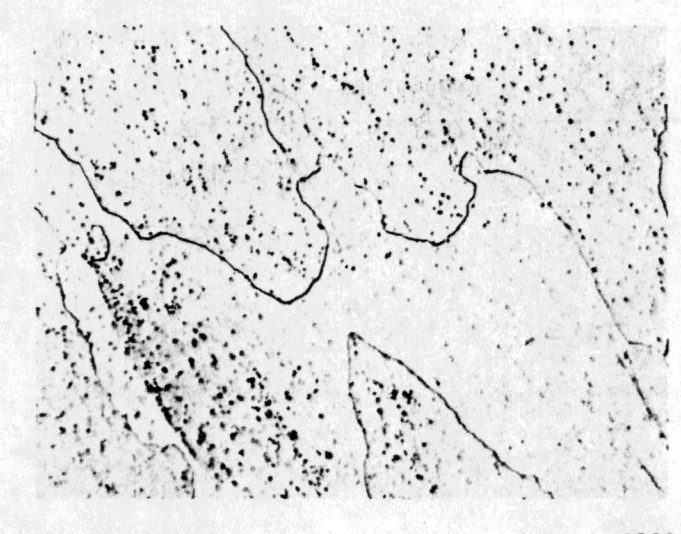


Bild 20a

Legierung: V-1Ti

Zustand: 1100°C, 3h/W



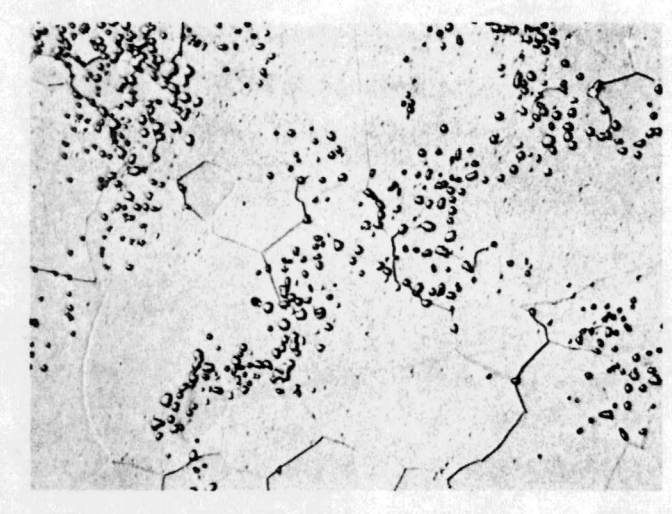


Bild 20b

Legierung: V-20Ti

Zustand: 1100°C, 3h/W





Bild 21a

Legierung: V-3Ti

Zustand: 1100°C, 3h/W +

600°C, 10d/W

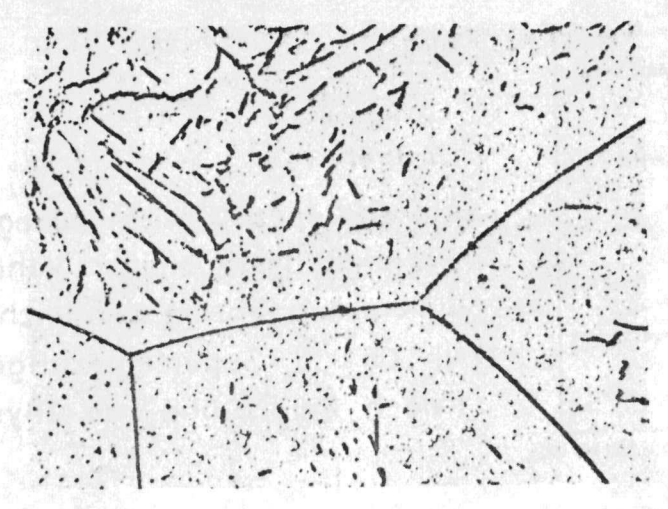


Bild 21b

Legierung: V-20Ti

Zustand: 1100°C, 3h/W +

700°C, 10d/W

× 1000

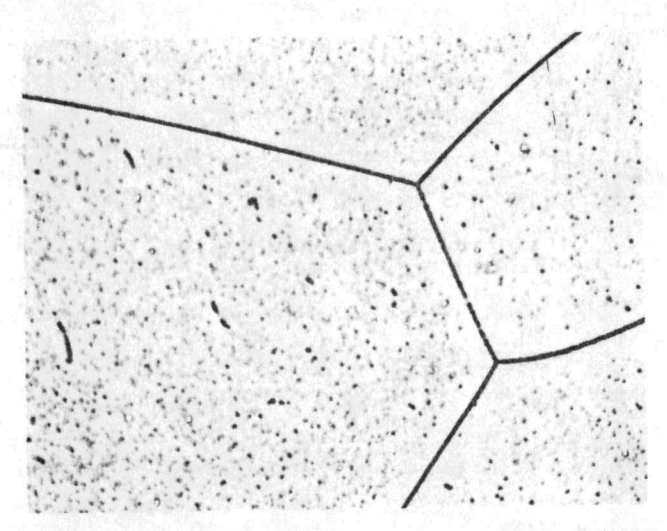


Bild 21c

Legierung: V-20Ti

Zustand: 1100°C, 3h/W +

400°C, 20d/W

× 1000

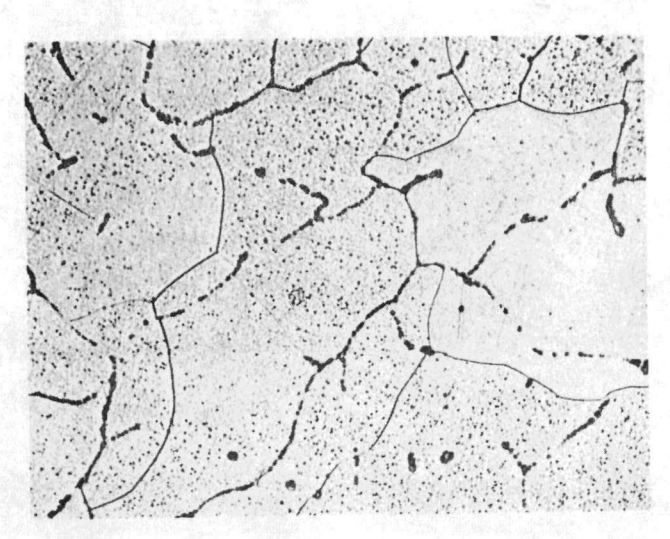


Bild 22

Legierung: V-2Zr + 800 ppm C Zustand: homog. + 600°C, 1d/W

x 500

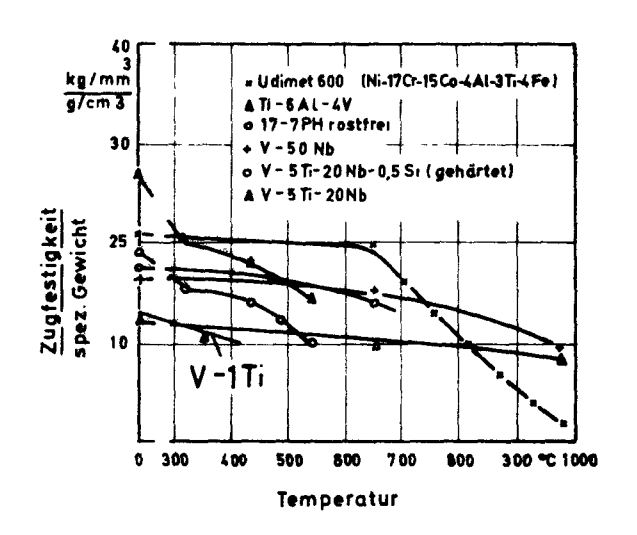


Bild 23

Auf das spez. Gewicht bezogene Warmfestigkeit einiger Vanadi – umlegierungen im Vergleich zu Ni – Cr – Co – Superlegierungen (nach Rajala und van Thyne) 10)